

Insights from Unplanned Outcomes in Laboratory DFIT Experiments for Utah FORGE Stimulation and Stress Analysis

Zhi Ye¹ and Ahmad Ghassemi²

1. Department of Geology and Geological Engineering, South Dakota School of Mines & Technology, SD, USA

2. Reservoir Geomechanics and Seismicity Research Group, The University of Oklahoma, Norman, OK, USA

ahmad.ghassemi@ou.edu

Keywords: Stress Measurement, Hydraulic Fracturing, DFIT, FORGE, Laboratory Experiments

ABSTRACT

Understanding the in-situ stress in the subsurface is crucial for many scientific and engineering activities, including the development of Enhanced Geothermal Systems (EGS). A common technique for determining the minimum principal stress is to interpret the pressure transient during a small-scale hydraulic fracturing test. A few hydraulic fracturing stress measurements have been conducted at Utah FORGE, and some results have shown discrepancies and posed challenges in interpretation. To address these issues, we conducted a series of controlled laboratory DFIT experiments, specifically tailored to the geothermal context of Utah FORGE (Ye & Ghassemi, 2023a, 2023b, 2024). Unlike previous studies, here we describe a set of laboratory DFIT experiments with unexpected results, and use them to shed light on the operational and interpretative aspects of hydraulic fracturing stress measurements in high-temperature and naturally fractured geothermal reservoirs. Specifically, we explore the effects of near-wellbore tortuosity, non-planar fracture geometry, injection rate, and cooling on the accuracy of hydraulic fracture stress measurements, aiming to enhance stress measurement accuracy and data interpretation at Utah FORGE and other geothermal reservoirs.

1. INTRODUCTION

Understanding the magnitudes and orientations of in-situ stress is critical for designing and optimizing subsurface engineering applications. Among the three principal stresses, the minimum principal stress (S_3 , or $S_{h\min}$ in most cases) is particularly significant as it controls fluid injection and re-injection conditions, governs the propagation of fluid-driven fractures, and influences the evolution of injection-induced seismicity. For deep formations, the magnitude of the minimum principal stress is typically measured using hydraulic fracturing (HF)-based tests, including minifrac tests, microfrac tests, and diagnostic fracture injection tests (DFITs) (Haimson & Fairhurst, 1967; McClellan & Roegiers, 1981; Hickman & Zoback, 1981). Although these tests have distinct definitions, they are often used interchangeably for small-scale stress measurements. In these tests, a small volume of pressurized fluid is injected into an isolated wellbore section, typically using a straddle packer system, to initiate and propagate a hydraulic fracture. The well is then shut in, and multiple injection and fall-off cycles may be performed to refine stress estimates. Throughout these cycles, wellbore pressure transients are monitored during both injection and shut-in phases to determine key pressure indicators.

The minimum principal stress is typically inferred from pressure indicators such as fracture reopening pressure (Bredehoeft et al., 1976; Shlyapobersky, 1989; Ito & Hayashi, 1993), instantaneous shut-in pressure (ISIP) (Hickman & Zoback, 1981; Gronseth & Kry, 1981), and fracture closure pressure (Castillo, 1987; Raaen et al., 2001; Barree et al., 2009; McClure et al., 2016, 2019). During the shut-in phase of a minifrac or DFIT, wellbore pressure rapidly declines until the fracture closes. The pressure decline curve is analyzed to determine the fracture closure pressure (P_c), which represents the minimum pressure required to keep a fracture open. This pressure is commonly assumed to be equal to the minimum principal stress, based on the linear relationship between fracture width and pressure (Gulrajani & Nolte, 2000). However, while HF-based tests are widely used for stress measurements in deep formations, accurately determining the minimum principal stress in deep geothermal reservoirs remains an ongoing research challenge. To address this, we conducted a series of laboratory DFIT experiments on large granite blocks (up to 17 × 17 × 17 inches) under true-triaxial stress and high-temperature conditions (up to 175°C) (Ye & Ghassemi, 2023a, 2023b, 2024). These experiments aimed to investigate the physics of fracture closure and the effects of cooling effect on stress determination.

The Utah FORGE project is developing a full-scale Enhanced Geothermal System (EGS) laboratory near Milford, Utah (Moore et al., 2020). A key research objective of FORGE is the accurate characterization of in-situ stress, which is crucial for the successful development of EGS in deep granitoid formations (>8,500 ft). The challenges associated with stress determination in this setting have drawn significant interest, as precise stress measurements are essential for optimizing stimulation strategies and ensuring the long-term viability of EGS development. As part of this effort, the Utah FORGE team has conducted a series of DFIT, micro-frac, and mini-frac tests in wells 58-32, 16A(78)-32, and 16B(78)-32. Most of these tests have produced consistent estimates of the minimum principal stress ($S_{h\min}$) within a reasonable range of 0.70-0.80 psi/ft (e.g., Nadimi et al., 2020; Xing et al., 2020; Xing et al., 2022; Kelley et al., 2023; Lu et al., 2023). However, some stress measurements have shown discrepancies in $S_{h\min}$ determination, such as the DFITs conducted in Zone 2 of well 58-32 in 2019 and the minifrac tests conducted in well 16B(78)-32, posing challenges in interpretation. Previous studies have suggested that these inconsistencies may be influenced by near-wellbore tortuosity, natural fractures, or borehole cooling effects (Nadimi et al., 2018; Xing et al., 2020; Kelley et al., 2023; Lu et al., 2023). In this study, we analyze a set of laboratory DFIT experiments that yield unexpected

results. Our findings provide additional insights that may help explain the variability observed in DFIT or mini-frac stress measurements at FORGE, enhancing the understanding of factors influencing stress determination in deep geothermal formations.

2. LABORATORY DFIT TESTS WITH UNEXPECTED RESULTS

2.1 Experimental Methods

The laboratory DFIT tests were conducted under controlled true-triaxial stress conditions using a novel, in-house high-temperature true-triaxial testing system (Hu & Ghassemi, 2020a; 2020b; Ye & Ghassemi, 2023a, 2023b, 2024), as illustrated in Figure 1(a). The samples were prepared as cubic blocks (Figure 1(b)), each with dimensions of $13 \times 13 \times 13$ inches (approximately $330 \times 330 \times 330$ mm). In the experiments, each cubic rock sample is subjected to true-triaxial stress compression along three orthogonal axes, as shown in Figure 1(c). An injection wellbore, 1-inch (25 mm) in diameter, was drilled into the center of each block from one of its side surfaces, as illustrated in Figure 1(d). This wellbore reached a depth of about roughly 6.5 inches (~ 165 mm). To effectively seal the gap between the injection tubing and the wellbore wall, high-strength epoxy was applied inside the wellbore. This procedure left an open section at the bottom of the wellbore, measuring about approximately 0.5 inch in length. A circular notch was also crafted at this open section to assist in initiating a fracture perpendicular to the minimum principal stress by fluid injection and minimizing the possible near-wellbore tortuosity.

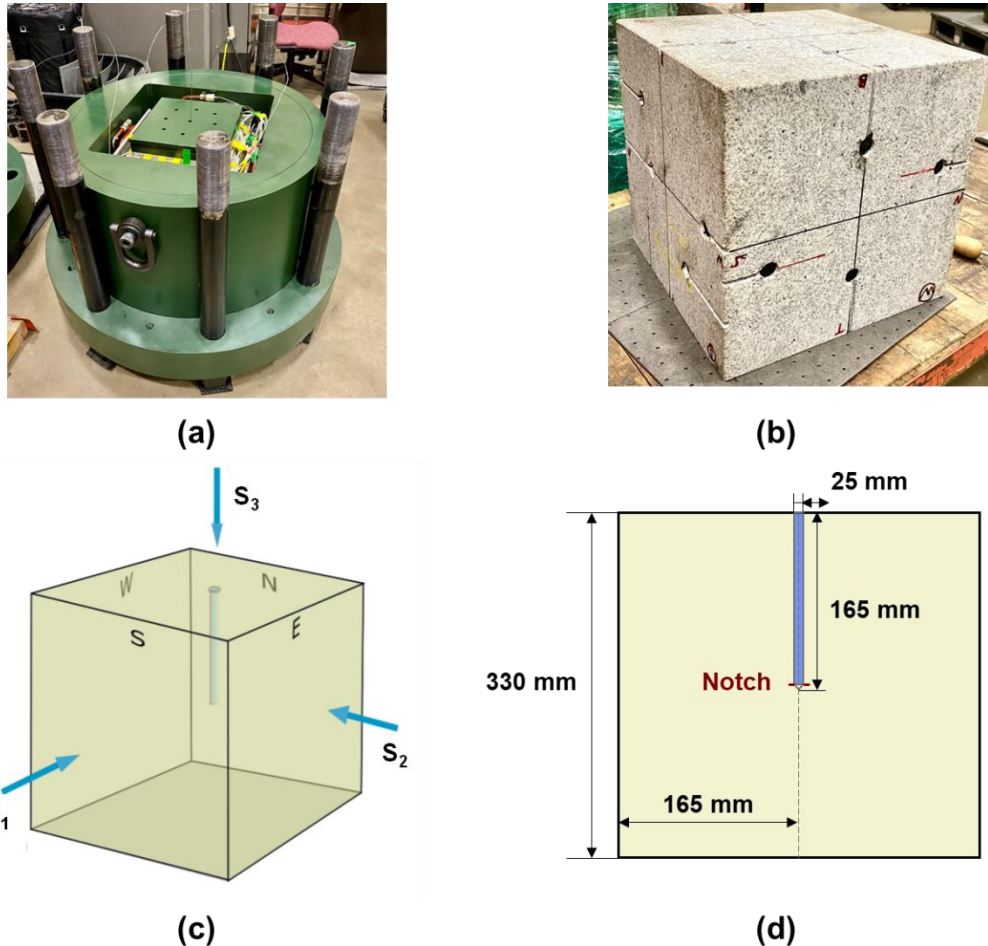


Figure 1: Experimental methods for laboratory DFIT Tests and stress measurements. (a) true-triaxial testing system; (b) A cubic rock sample of Sierra White Granite, measuring $13 \times 13 \times 13$ inches in size; (c) the cubic rock sample subjected to controlled true-triaxial stress conditions; (d) layout depicting the placement of an injection wellbore within the cubic rock sample.

The experiment was designed to simulate field-scale DFIT tests, incorporating hydraulic fracture initiation, propagation, and multiple injection/fall-off cycles. Wellbore pressure and injection parameters were continuously monitored to assess stress conditions. These measurements were then compared with the applied minimum principal stress (s_3) to evaluate the accuracy of hydraulic fracturing (HF)-based stress estimation. The laboratory DFIT procedure consisted of three main steps: (1) True-Triaxial Loading: Each cubic rock sample was subjected to a controlled true-triaxial stress state using an in-house true-triaxial testing system. Precise stress control was essential for reliable stress interpretation in subsequent injection/fall-off tests. To ensure accuracy, the flat jacks used for stress application were calibrated with a load cell before testing, maintaining an applied stress error below 1%. Once the target stress levels were achieved, the stress state was held stable for several hours to establish a consistent reference. (2) Hydraulic Fracturing: A hydraulic fracture was initiated and propagated within the stressed rock sample to simulate DFIT conditions. This was achieved by injecting deionized water at a constant flow rate through a pre-drilled injection wellbore. A circular notch at the wellbore opening guided the fracture to propagate perpendicular

to the applied minimum principal stress (S_3). To ensure controlled fracture growth, a pressure drop threshold of 69–138 kPa (10–20 psi) was maintained, preventing excessive extension. Acoustic emission (AE) monitoring was used to verify fracture propagation. This approach aims to result in a sufficiently large, planar fracture (at least 30 times the wellbore area) with minimal near-wellbore tortuosity, allowing for accurate stress analysis in subsequent tests. (3) Injection/Fall-off Tests: Following fracture creation, a series of injection/fall-off cycles were conducted to evaluate fracture closure behavior under controlled conditions. The same fluid used in Step 2 was reinjected to reopen the fracture, followed by well shut in. Wellbore pressure and AE signals were continuously recorded during both injection and shut-in phases to facilitate stress interpretation.

The experimental methods used in our laboratory study allowed for a systematic investigation of fracture closure dynamics and provided valuable insights into HF-based stress measurement techniques under controlled conditions. While most laboratory DFIT tests produced expected results—such as planar fractures, well-defined signatures of fracture reopening and closure, and stress estimates consistent with the applied minimum principal stress (S_3)—a few experiments yielded unexpected outcomes. These anomalies included significant discrepancies in stress measurements that deviated from the applied stress, as well as cases where pressure breakdown and/or fracture reopening lacked clear signatures. Such unexpected results highlight the complexity of hydraulic fracturing behavior and suggest potential factors influencing stress measurement interpretations. Understanding these deviations is essential for improving the reliability of DFIT-based stress characterization, particularly in field applications such as Utah FORGE. In the following sections, we examine specific laboratory experiments that may provide insights into similar challenges encountered in FORGE stress measurements.

2.2 Test 1 on Sierra White Granite

The first test (Test 1) we present was conducted on a Sierra White granite block with dimensions of $330 \times 330 \times 330$ mm (approximately $13 \times 13 \times 13$ inches). The relevant geomechanical properties of Sierra White granite are as follows: Young's modulus ($E = 67$ GPa), Poisson's ratio ($\nu = 0.32$), uniaxial compressive strength ($UCS = 150$ – 210 MPa), internal friction angle ($\phi = 46^\circ$), and tensile strength ($T = 11$ MPa). Additionally, this granite has an extremely low permeability, ranging from 5×10^{-19} m 2 to 1×10^{-18} m 2 . X-ray diffraction (XRD) analysis indicates that the granite is primarily composed of Quartz (43.5%) and Albite (46.1%) by weight, with minor amounts of Sanidine (4.8%), Biotite (2.7%), Illite (2.0%), and Clinochlore (0.9%). The true-triaxial stress applied to the block was set as $S_1 = 1500$ psi, $S_2 = S_3 = 1000$ psi, as illustrated in Figure 1(c). As described in Section 3.1, a notch was introduced at the bottom of the injection wellbore to promote hydraulic fracture propagation perpendicular to the applied minimum principal stress (S_3).

During the experiment, an initial hydraulic fracturing cycle was conducted to create a fracture, followed by three injection/fall-off tests to measure stress. The injection records, including wellbore pressure and injection rate, are illustrated in Figure 2.

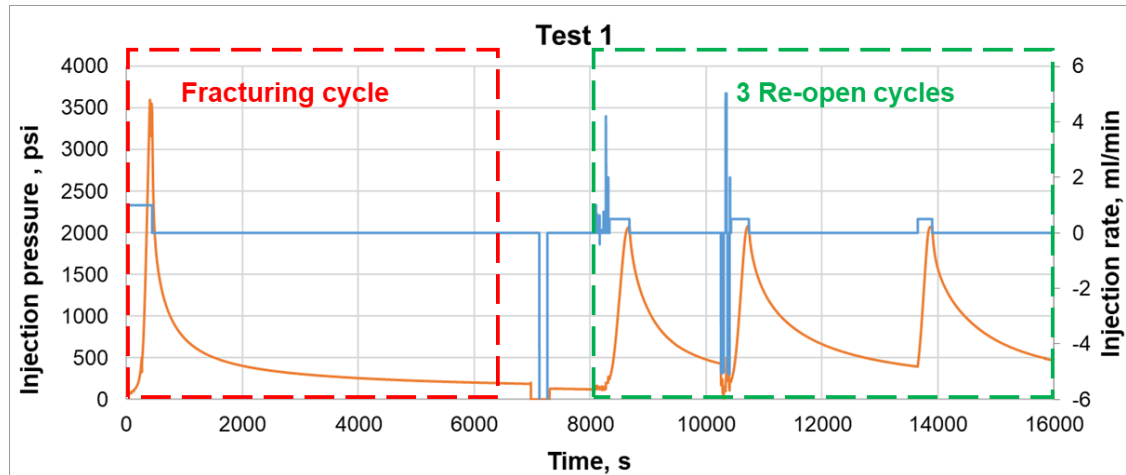


Figure 2: Wellbore pressure and injection rate records for Test 1, showing one hydraulic fracturing cycle followed by three injection/fall-off cycles.

During hydraulic fracturing, deionized water was injected at a constant rate of 1 ml/min to create a hydraulic fracture. As shown in Figure 3, the pressure curve exhibits an unusual two-phase breakdown behavior. The first breakdown occurs at approximately 3599 psi, followed by a brief pressure drop and a second breakdown at 3553 psi. This observation suggests two distinct phases of fracture propagation, which is uncommon in standard hydraulic fracturing tests. The two-phase behavior observed during the hydraulic fracturing cycle of Test 1 suggests that uncommon dynamics occurred during the process. The first peak in the pressure curve likely represents an initial phase where the fracture begins to initiate and propagate near the wellbore. The brief pressure drops following this initial peak suggests a temporary stabilization or limited extension of the initial fracture before the pressure builds up again. The second peak, reaching 3553 psi, corresponds to the full propagation of the hydraulic fracture. At this stage, the applied pressure overcomes the system's resistance, allowing the fracture to propagate further from the wellbore. This transition from near-wellbore initiation to full-scale propagation reflects the complexity of Test 1, which is distinct from the majority of laboratory DFIT tests we have conducted, where the breakdown pressure typically exhibits a single and clear peak (Ye & Ghassemi, 2023a; 2023b, 2024).

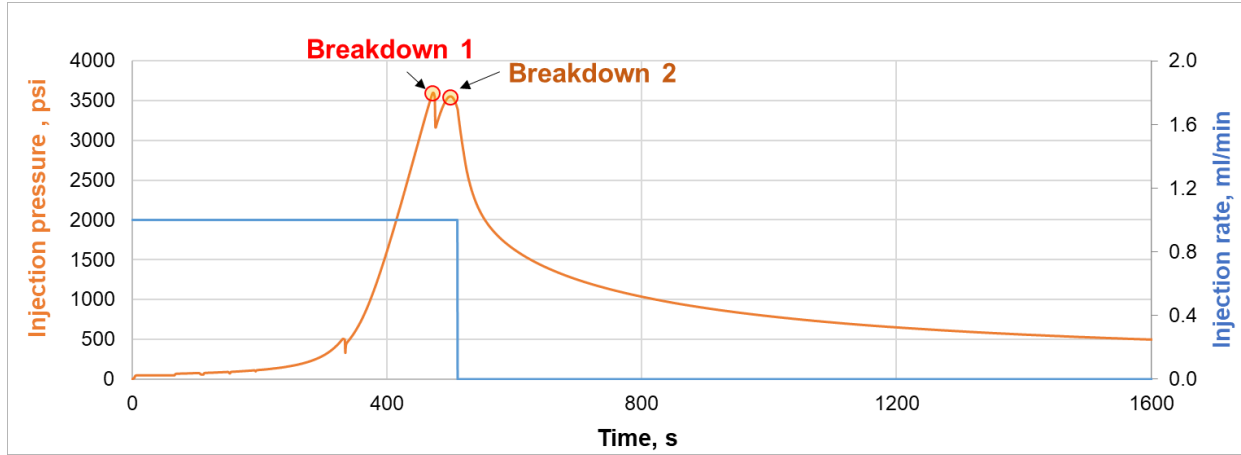


Figure 3: Wellbore pressure and injection rate records of the hydraulic fracturing cycle for Test 1, showing an uncommon pressure transients with two-phase behavior.

The two-phase fracture propagation behavior observed in the experiment can be explained by several factors: natural rock heterogeneities, pre-existing microcracks, and near wellbore issues such as stress concentration around the notch. First, natural heterogeneities in the rock, such as variations in mineral composition, grain size, or mechanical properties, can create localized zones of weakness or stress concentration. These variations can influence how the fracture initiates and propagates, leading to an initial phase of localized fracture growth before full-scale propagation occurs. Second, pre-existing microcracks within the rock may significantly affect fracture dynamics. These microcracks can act as stress concentrators and may partially open or propagate under applied pressure. This localized behavior can cause the fracture to initiate in a non-uniform manner, resulting in the observed initial pressure peak followed by a temporary drop. Finally, stress concentration around the notch at the wellbore opening is another key factor. The notch is designed to direct the fracture perpendicular to the applied minimum principal stress (S_3). However, variations in the geometry or placement of the notch could lead to uneven stress distribution, influencing how and when the fracture initiates. This may explain the initial phase of localized fracture propagation before the pressure builds to the breakdown point for full-scale propagation.

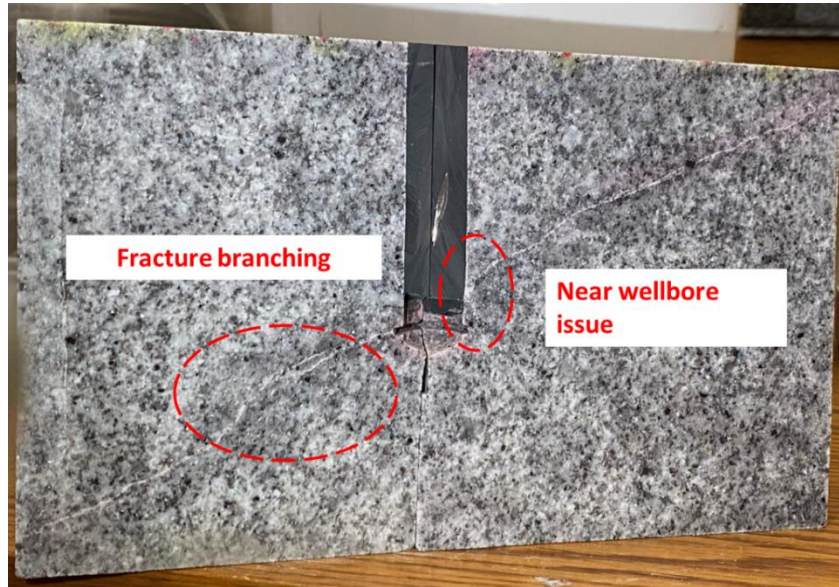


Figure 4: Complex fracture geometry of the hydraulic induced fracture in Test 1.

The unexpected fracture propagation is further clarified by the geometry of the created hydraulic fracture. After the experiment, the hydraulic fractured Sierra White Granite block was cut and sliced by a diamond saw to examine the fracture geometry. Two critical features, fracture branching and significant near-wellbore issue, observed in the fracture geometry (Figure 4) are responsible for the unexpected fracture propagation and the uncommon pressure record seen in the laboratory hydraulic fracturing test. The observed fracture branching, evident in the left portion of Figure 4, indicates non-planar and irregular fracture propagation. This behavior is uncommon in laboratory hydraulic fracturing tests, where fractures typically propagate as single, planar features aligned perpendicular to the minimum principal stress (S_3), such as in most laboratory hydraulic fracturing tests (Hu & Ghassemi, 2020a; Ye & Ghassemi, 2023a, 2023b). The branching likely corresponds to the initial pressure peak observed in the pressure record, where the fracture began to propagate unevenly during the early phase of the test. While fracture branching could be attributed to natural heterogeneities or the presence of microcracks

in the rock, prior SEM analysis of Sierra White Granite thin sections (Ye & Ghassemi, 2018) suggests that this granite is generally homogeneous, with evenly distributed grains and crystal sizes. Consequently, we attribute the fracture branching more likely to the influence of pre-existing microcracks, which may have acted as stress concentrators, redirecting the fracture path and resulting in irregular propagation. Additionally, near-wellbore damage and complexity, marked as "near wellbore issues" in the image, provide further evidence of the unusual dynamics observed during the experiment. The notch, designed to direct the fracture perpendicular to S_3 , may have introduced uneven stress concentrations near the wellbore. These stress concentrations likely contributed to localized instability and unintended fracture initiation near the wellbore. This behavior aligns with the temporary pressure drop observed in the pressure record following the first peak, as the fracture encountered resistance and instability before transitioning to full-scale propagation. Notably, the right wing of the hydraulic fracture did not initiate directly from the notch as expected but rather began approximately one inch above the notch. This deviation from the intended fracture path underscores the complexity that can arise during HF-based stress measurements. Although the exact cause of this behavior could be more complicated, it may involve a combination of factors, including rock type, the presence of natural fractures, injection parameters, and operational conditions. This unexpected outcome highlights the need to account for such complexities in both laboratory and field-scale hydraulic fracturing tests, as they can significantly impact the interpretation of stress measurements and fracture behavior.

After completing the experiments, the fracture coordinates were meticulously measured, and the fracture geometry was reconstructed in both two-dimensional and three-dimensional views, as shown in Figure 5. The reconstructed geometry indicates that the overall fracture angle relative to S_3 (the vertical axis) is approximately 60°. At this angle, the normal stress acting on the fracture is calculated to be close to 1366 psi. This deviation in fracture orientation from the expected alignment with the principal stresses corresponds closely with the unexpected pressure records observed during the hydraulic fracturing cycle.

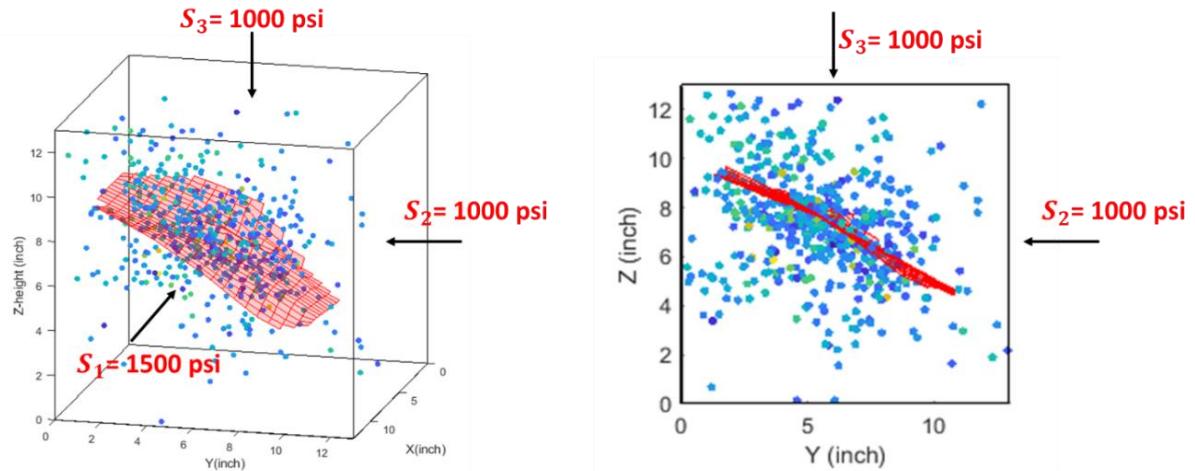


Figure 5: Reconstruction of fracture geometry in test 1.

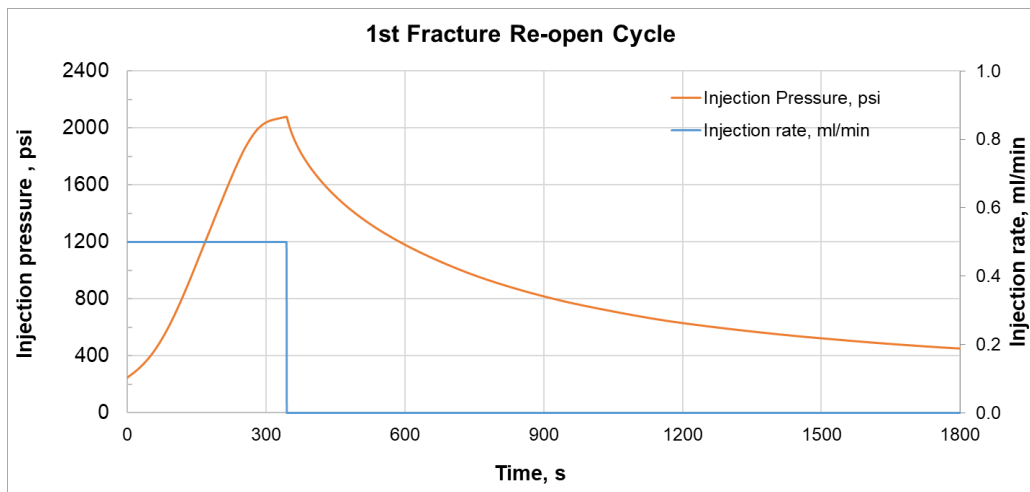


Figure 6: Pressure and flow rate record of the first injection/falloff cycle in Test 1.

As a result of the unexpected fracture geometry, coupled with the observed fracture branching and near-wellbore issues, the stress measurements during the three injection/falloff tests were likely influenced by the irregular fracture propagation, leading to elevated stress estimates. To further explore this, we analyzed the pressure transients from the three injection/falloff cycles. Using the first injection/falloff

cycle as an example, as shown in Figure 6, a notable deviation in the pressure behavior can be observed. The first unusual observation is the continuous pressure increase after a significant deflection in the pressure curve. This deflection is typically interpreted as the reopening of the fracture, where increased fluid flow into the fracture would generally result in a clear pressure drop as the fracture begins to open further. However, in Test 1, instead of the expected pressure drop, the pressure continues to rise even after the fracture reopening. This behavior likely reflects increased resistance to fluid flow within the unexpected fracture features, which could be attributed to the complex fracture geometry observed in this test. Specifically, the continuous pressure rise may indicate the presence of significant fracture branching or tortuosity near the wellbore, which restricts fluid flow and increases the pressure required to sustain fracture reopening and propagation. Additionally, the deviation of the fracture orientation from the expected alignment with S3 and the near-wellbore damage observed in the experiment could further compound this resistance, causing the pressure to remain elevated. This behavior is consistent with the earlier observations of fracture geometry and branching, reinforcing the link between fracture geometry and morphology and the pressure response.

We further interpreted the three pressure indicators—fracture reopening pressure, *ISIP*, and fracture closure pressure—to determine the stress and compared these values to the applied stress. It is important to note that the stresses reflected by these pressure indicators do not represent the minimum principal stress but rather the normal stress acting on the fracture, as the created fracture is not perpendicular to the applied minimum principal stress (Figure 5). As shown in Figure 7, the fracture reopening pressure (1945 psi) is significantly higher than the estimated normal stress acting on the fracture (1366 psi). Similarly, the *ISIP* is estimated at 1748 psi, which, while lower than the fracture reopening pressure, is still approximately 382 psi higher than the expected normal stress. Interestingly, in most DFIT studies, including our previous laboratory experiments, the *ISIP* is generally observed to be higher than the fracture reopening pressure. This deviation in Test 1 may be attributed to a large stress concentration near the wellbore, caused by the observed near-wellbore issues. These stress concentrations likely restrict the fracture's ability to reopen under normal conditions, requiring higher pressures to overcome the resistance. This behavior further highlights the influence of near-wellbore complexity on fracture propagation and stress measurements, distinguishing this test from conventional DFIT results.

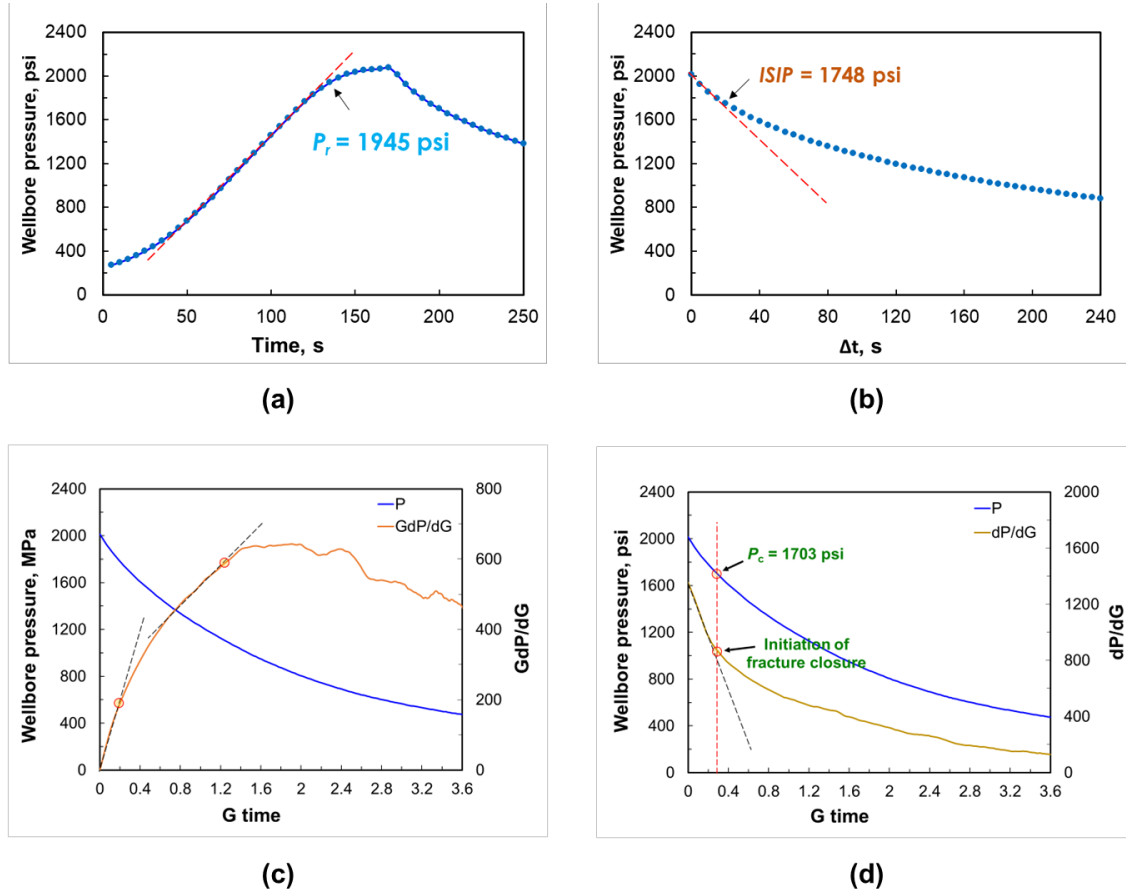


Figure 7: Stress interpretation using (a) fracture reopening pressure, (b) *ISIP*, (c) fracture closure pressure determined from the GdP/dG curve using the tangent method, and (d) fracture closure pressure determined from the dP/dG curve.

On the other hand, we also attempted to interpret the fracture closure pressure using two widely adopted methods: the "tangent method" and the "compliance method." However, neither method provided good estimates of fracture closure pressure for Test 1 with unexpected fracture geometry. Using the tangent method, it was difficult to identify a clear deflection point on the GdP/dG vs. G curve, making fracture closure interpretation challenging. Similarly, the compliance method based on the dP/dG vs. G curve that showed a monotonic decrease, failing to present a distinct signature for determining fracture closure. Alternatively, we applied the first deviation on the dP/dG

vs. G curve, as suggested by Ye & Ghassemi (2024), to estimate the initiation of mechanical fracture closure. This approach yielded a fracture closure pressure of 1703 psi, which is the closest estimate to the expected value. However, it is still 337 psi higher than the calculated normal stress acting on the fracture. These discrepancies further highlight the challenges posed by the unexpected fracture

The high stress estimates observed in this experiment are often attributed to "near-wellbore tortuosity," a phenomenon commonly reported in field DFIT tests. In such cases, irregular fracture initiation and propagation near the wellbore result in anomalously high-pressure responses. However, the findings from this laboratory DFIT test suggest that the unexpected high stress estimates may not be solely linked to near-wellbore issues. The unusual fracture geometry, characterized by branching and deviation from a perpendicular alignment to the minimum principal stress (S_3), appears to also play a significant role in influencing the pressure responses and stress measurements. Additionally, as shown by the fracture branching in Figure 4, tortuosity due to irregular fracture propagation can occur not only near the wellbore but also farther away from it. These findings emphasize the importance of considering both near-wellbore effects and fracture geometry when interpreting stress estimates from DFIT tests, as both factors can contribute to overestimated stress values.

2.3 Test 2 on Scioto Sandstone

The second laboratory DFIT test (Test 2) was conducted on a Scioto Sandstone block with extremely high permeability (100–400 microDarcy). The sample size, preparation, and testing procedure for Test 2 were similar to those used in Test 1, with only two notable differences: the applied stress conditions and the injection rate. For Test 2, the applied stress conditions included a minimum principal stress of 1250 psi, an intermediate principal stress of 2000 psi, and a maximum principal stress of 3000 psi. Due to the high permeability of the Scioto Sandstone, a higher injection rate of 10–40 ml/min ($3.5\text{--}14 \times 10^{-4} \text{ ft}^3/\text{min}$) was required to initiate and propagate a hydraulic fracture. The injection rate was stepwise increased from 10 ml/min to 40 ml/min to create a hydraulic fracture in the Scioto Sandstone block, as shown in Figures 8(a) and 8(b). The breakdown pressure was recorded at 2754 psi. The created fracture was predominantly planar, as illustrated in Figure 8(c). To visualize the fracture, fluorescent particles were injected into the sample, and the block was split open after the experiment, revealing a well-defined hydraulic fracture surface.

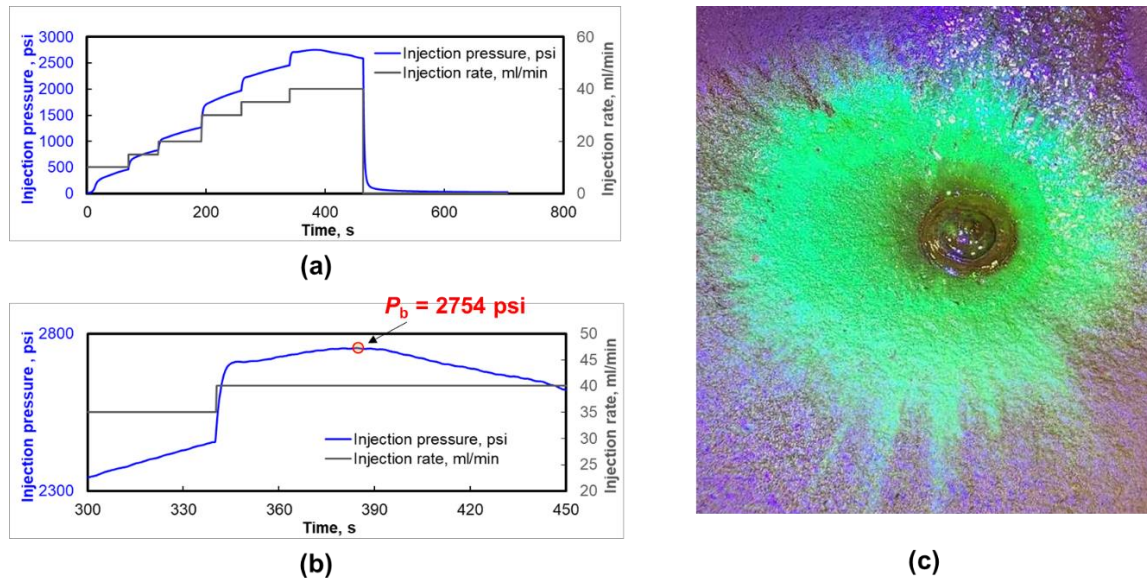


Figure 8: Hydraulic fracturing cycle of Test 2 conducted on high-permeability Scioto Sandstone. (a) Full pressure and injection rate records; (b) Zoomed-in view clearly showing the breakdown pressure during hydraulic fracturing; (c) Fracture surface highlighted with fluorescent dye, illustrating a nearly planar fracture.

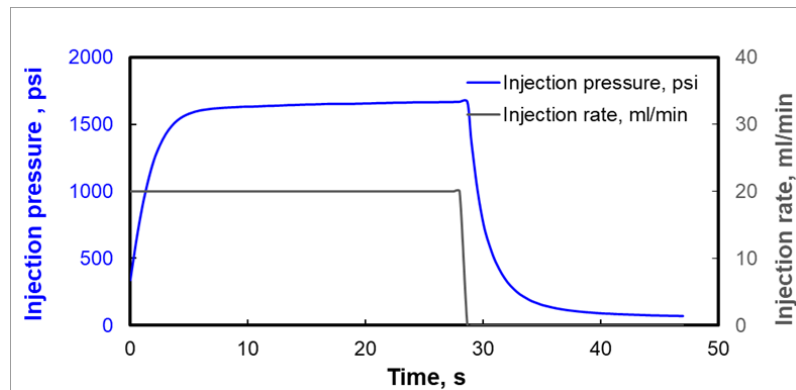
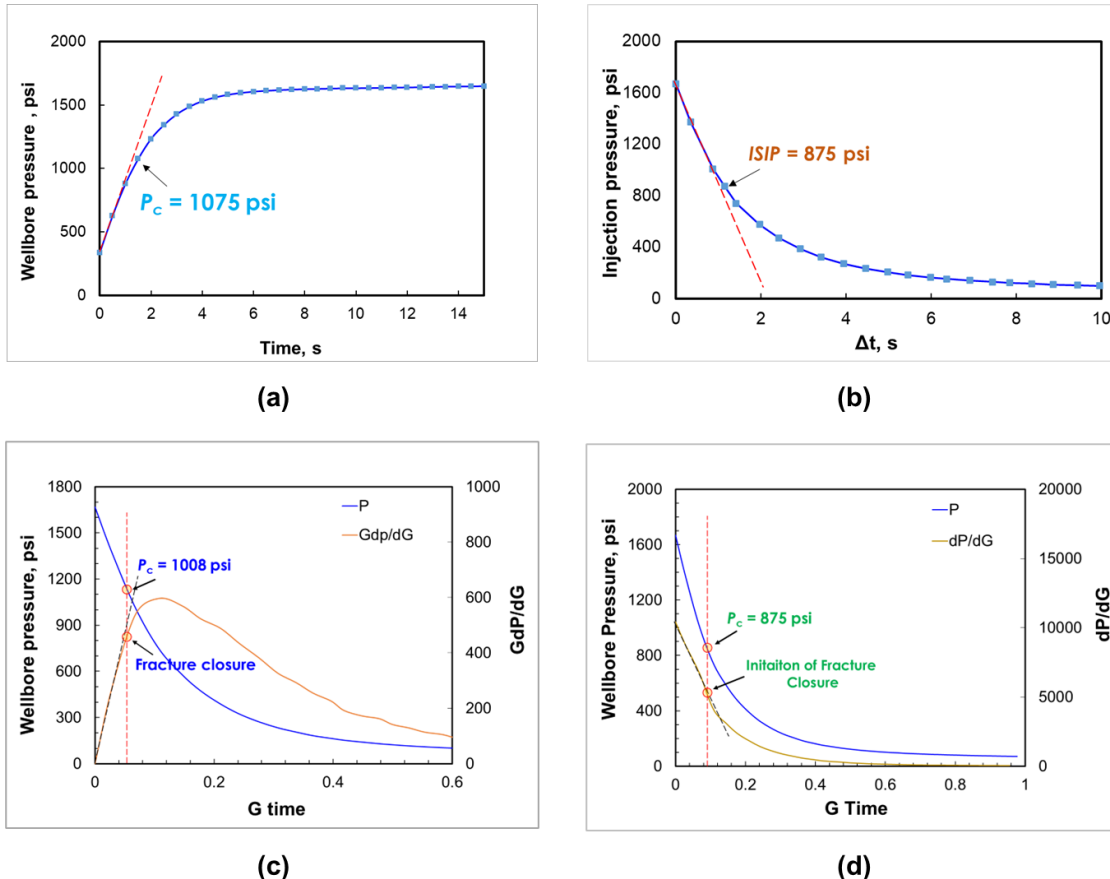


Figure 9: Pressure and injection rate record for an injection/falloff cycle conducted at a relatively low injection rate of 20 ml/min.

Following the hydraulic fracturing cycle, a series of injection/falloff tests were conducted to measure stress. Most injection/falloff cycles conducted with a higher injection rate, above 30 ml/min, yielded reasonable stress estimates that were consistent with the applied minimum principal stress (S_3) of 1250 psi (Ye & Ghassemi, 2024). This consistency can be attributed to the creation of a nearly planar hydraulic fracture, ensuring that the normal stress acting on the fracture closely aligns with the applied S_3 of 1250 psi. However, some unexpected results were observed when lower injection rates were used. Specifically, at injection rates below 30 ml/min, the hydraulic fracture did not fully reopen, as evidenced by the pressure records. Figure 9 shows an injection/falloff cycle conducted at a relatively low injection rate of 20 ml/min. The pressure reaches a steady state rather than exhibiting the characteristic pressure drop typically associated with successful fracture reopening. This steady state suggests that the injected fluid, in this case, deionized water, continuously leaks into the rock matrix without creating sufficient pressure to overcome the resistance needed to reopen the fracture. If the fracture had reopened, a significant pressure drop would have been observed, corresponding to the increased fluid flow into the fracture. The absence of this pressure drop in the record supports the conclusion that the fracture remained closed under these conditions. As a result, if the pressure transients of the injection/falloff cycle indicate that the fracture did not reopen, the resulting stress estimates would likely be underestimated.

Figure 10 provides a detailed interpretation of stress based on fracture reopening pressure, $ISIP$, and closure pressure from the injection/falloff cycle conducted at a low injection rate. As shown, the fracture reopening pressure is approximately 1075 psi, which is 175 psi lower than the applied minimum principal stress (S_3) of 1250 psi. Similarly, the $ISIP$ is estimated to be 875 psi, significantly lower than the expected S_3 by 375 psi. The pressure response also demonstrates normal leakoff behavior. The estimated fracture closure pressure, determined using the "tangent method," is 1008 psi, which is still 242 psi lower than the applied S_3 . Additionally, the compliance method does not provide a distinct signature for fracture closure, as the pressure continues to decrease monotonically. Using the first deviation on the dP/dG vs. G curve, the fracture closure pressure is estimated to be 875 psi, which is substantially lower than the applied stress. These results indicate that the low injection rate likely impacted the fracture's ability to fully reopen, resulting in underestimated stress values across all pressure indicators. The consistently lower stress estimates highlight the critical role of injection rate in ensuring accurate stress interpretation and reliable fracture behavior. The discrepancy between the pressure indicators and the applied stress further underscores the importance of maintaining appropriate injection parameters during DFIT testing to achieve fracture reopening and ensure reliable stress measurements during DFIT tests.

**Figure 10: Stress interpretation using (a) fracture reopening pressure, (b) ISIP, (c) fracture closure pressure determined from the GdP/dG curve using the tangent method, and (d) fracture closure pressure determined from the dP/dG curve.**

On the other hand, when a higher injection rate was used, a clear pressure drop was observed, indicating full fracture reopening. As illustrated in Figure 11, during an injection/falloff cycle conducted at an injection rate of 35 ml/min, the pressure initially increased as fluid was injected into the fracture. Upon reaching a peak, the pressure dropped sharply, signifying the moment the fracture fully reopened and fluid began to flow more freely into the fracture. This pressure drop confirms that the fracture was successfully reopened, allowing accurate stress interpretation (Ye & Ghassemi, 2024). Unlike the injection/falloff cycle at lower injection rates (Figure 9), where the absence of a pressure drop suggested incomplete reopening, the results from Figure 11 reinforce the importance of using a sufficiently high injection rate to ensure fracture reopening and reliable stress measurements.

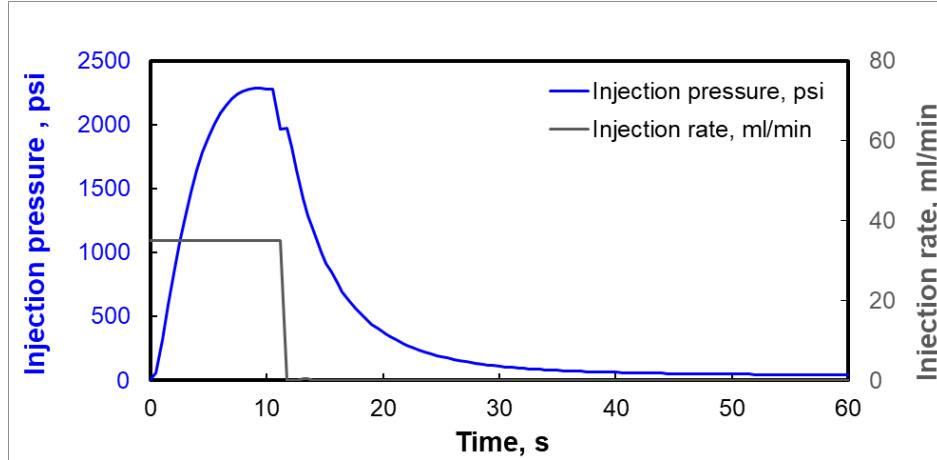


Figure 11: Pressure and injection rate record for an injection/falloff cycle conducted at a higher injection rate of 35 ml/min, illustrating a distinct pressure drop upon fracture reopening.

3. DISCUSSIONS AND INSIGHTS ON FORGE DFIT TESTS

Hydraulic fracturing-based stress measurement is essential for many subsurface engineering operations, including the development of Enhanced Geothermal Systems (EGS), which depend on creating efficient fracture networks to enhance permeability through hydraulic stimulation. At the Utah FORGE initiative, a series of DFIT (Diagnostic Fracture Injection Tests) and micro-frac tests have been successfully conducted for stress measurement in well 58-32 and well 16A(78)-32. Most of these tests have produced consistent and reasonable stress estimates, with the minimum principal stress ($S_{h\min}$) typically ranging from 0.70 to 0.80 psi/ft.

However, the DFIT tests conducted in Zone 2 of well 58-32 in 2019 yielded a significantly higher $S_{h\min}$ estimate of 0.80–0.95 psi/ft. Several possible explanations for these elevated stress measurements have been suggested, including “back stress” (a proxy for poroelastic effects) or high near-wellbore tortuosity (Xing et al., 2019), and extension of a natural fracture instead of initiation of a hydraulic fracture or interactions between hydraulic and natural fractures (Kamali and Ghassemi, 2019). This interaction increases local stress, contributing to the higher closure stress observed in Zone 2. Our laboratory Test 1, which exhibited unexpected fracture geometry, supports this possibility. In Test 1, the possible presence of pre-existing microcracks (analogous to natural fractures in the field) led to irregular fracture propagation and branching. Additionally, fracture geometry deviating from the expected perpendicular orientation to the applied minimum principal stress, along with near-wellbore issues, likely also contributed to overestimated stress values. Our results highlight the critical importance of operational control in hydraulic fracturing-based stress measurements. Ensuring proper fracture initiation and controlling propagation pathways are essential to minimize the influence of natural fractures, near-wellbore complexities, and unexpected fracture geometries on stress estimates. Such measures are important for improving the reliability and accuracy of stress measurements in geothermal systems and other subsurface applications.

Furthermore, a series of mini-frac tests conducted in well 16B(78)-32 yielded unexpectedly low stress measurements, ranging from 0.49 to 0.60 psi/ft (Kelley et al., 2023). These values are significantly lower than the stress estimates from wells 58-32 and 16A(78)-32, which ranged from 0.70 to 0.80 psi/ft (e.g., Xing et al., 2020). Researchers have suggested that this discrepancy may be due to borehole cooling, as cold fluid was circulated through surface chillers before the mini-frac tests (Kelley et al., 2023; Lu et al., 2023). Cooling likely caused thermal contraction of the rock, reducing the measured stress. To correct for this effect, some have proposed adding 0.2 to 0.3 psi/ft to the recorded stress values. Our previous experimental studies (Ye & Ghassemi, 2023b) have shown that cooling can lead to underestimated S_3 values. However, the extent of this effect depends on the injection rate. If the injection rate is too low, cooling may have less impact than expected. In our lab experiments, we used relatively high injection rates to amplify the cooling effect. However, in field conditions, the impact is likely smaller because injection fluids typically heat up as they enter the formation. Additionally, the injection rates used in HF-based stress measurements are generally much lower than those used in stimulation treatments, leading to smaller temperature differences. Most mini-frac tests in well 16B(78)-32 were conducted at very low injection rates (0.002–0.015 bpm), much lower than the 8–15 bpm used in the 2017 and 2019 DFITs in well 58-32, and also far below the 0.5–5 bpm used in the 2021 micro-frac and DFIT tests in well 16A(78)-32. This extremely low injection rate was likely insufficient to fully initiate or reopen a hydraulic fracture. In fact, out of seven mini-frac tests, only the second test (MF-2) may have successfully created a hydraulic fracture, while the rest did not show a clear breakdown event. Pressure transients from these tests showed characteristics similar to those observed in the low-injection-rate DFIT cycle of Test 2 (Figure 9), where a pressure plateau indicated incomplete fracture reopening. If the fracture does not fully reopen, the

recorded pressures will underestimate the actual stress, resulting in lower stress measurements. Additionally, geological factors, such as the density and orientation of natural fractures in the tested zone, may have also influenced the results. Under low injection rates, relatively permeable natural fractures could have taken up most of the injected fluid, further limiting the ability to initiate or reopen a hydraulic fracture for stress measurements. In naturally fractured reservoirs, achieving accurate stress measurements requires a higher injection rate to ensure the creation and full reopening of a hydraulic fracture.

4. CONCLUSIONS

Accurate stress measurements are essential for optimizing subsurface engineering operations, particularly in Enhanced Geothermal Systems (EGS), where effective hydraulic stimulation depends on precise stress characterization. Through unexpected laboratory DFIT tests and analysis of field data from the Utah FORGE initiative, this study provides additional insights into factors influencing stress measurements in deep geothermal formations. Our laboratory experiments revealed that unexpected fracture behaviors, such as branching and deviations in geometry, can significantly impact stress estimates. Test 1 demonstrated that pre-existing microcracks, near-wellbore issues, and complex fracture geometry can lead to overestimated stress values. These findings align with observations from Zone 2 of well 58-32, where higher stress estimates were attributed to the interaction between hydraulic and natural fractures. This highlights the importance of controlling fracture propagation during HF-based stress measurements to minimize non-planar fractures and near-wellbore complexities, ensuring more accurate stress interpretation. Conversely, Test 2 on Scioto Sandstone showed that low injection rates can result in incomplete fracture reopening, leading to underestimated stress values. This behavior was also observed in mini-frac tests from well 16B(78)-32, where insufficient injection rates likely contributed to anomalously low stress estimates, in addition to the original proposed cooling effect. Overall, this study highlights the critical role of operational and geological factors, including fracture geometry, near-wellbore conditions, injection rates, and thermal effects, in determining the reliability of stress measurements.

REFERENCES

Barree, R. D., Barree, V. L., & Craig, D. P. (2009). Holistic fracture diagnostics: consistent interpretation of prefrac injection tests using multiple analysis methods. *SPE Production & Operations*, 24(03): 396-406.

Bredehoeft, J. D., Wolff, R. G., Keys, W. S., & Shuter, E. (1976). Hydraulic fracturing to determine the regional in situ stress field, Piceance Basin, Colorado. *Geological Society of America Bulletin*, 87(2), 250-258.

Castillo, J. L. (1987). Modified fracture pressure decline analysis including pressure-dependent leakoff. In *SPE/DOE Joint Symposium on Low Permeability Reservoirs, Denver, Colorado, USA*.

Gronseth, J. M., & Kry, P. R. (1981). Instantaneous shut-in pressure and its relationship to the minimum in-situ stress. *Hydraul Fract Stress Meas*, 139, 147-166.

Gronseth, J. M., & Kry, P. R. (1981). Instantaneous shut-in pressure and its relationship to the minimum in-situ stress. *Hydraul Fract Stress Meas*, 139, 147-166.

Haimson, B., & Fairhurst, C. (1967). Initiation and extension of hydraulic fractures in rocks. *Society of Petroleum Engineers Journal*, 7(03), 310-318.

Hickman, S. H., & Zoback, M. D. (1981). The interpretation of hydraulic fracturing pressure-time data for in situ stress determinations. In *Workshop on Hydraulic Fracturing Rock Stress Measurements; National Academy Press: Washington, DC, USA* (pp. 103-127).

Hu, L., & Ghassemi, A. (2020b). Heat production from lab-scale enhanced geothermal systems in granite and gabbro. *International Journal of Rock Mechanics and Mining Sciences*, 126, 104205.

Hu, L., Ghassemi, A., Pritchett, J., & Garg, S. (2020a). Characterization of laboratory-scale hydraulic fracturing for EGS. *Geothermics*, 83: 101706.

Ito, T., & Hayashi, K. (1993, December). Analysis of crack reopening behavior for hydrofrac stress measurement. In *International journal of rock mechanics and mining sciences & geomechanics abstracts* (Vol. 30, No. 7, pp. 1235-1240). Pergamon.

Kamali, A., and Ghassemi, A.: DFIT considering complex interactions of hydraulic and natural fractures, Proceedings, SPE Hydraulic Fracturing Technology Conference and Exhibition (2019).

Kelly, M., Raziperchikolaee, S., Likrama , F., et al. (2023). Milestone 3.4 Report (In-Situ Measurement of Stress). Utah FORGE Project 2-2439.

Lu, G., Lu, Y., Kelley, M., Raziperchikolaee, S., & Bunger, A. Interpretation of Mini-frac Test Data Accounting for Wellbore Cooldown in an EGS Well at the Utah FORGE Site: A Numerical Study. *Proceedings of 2023 Geothermal Rising Conference, Reno, Nevada*, October 1-3.

McClure, M., et al. (2019). A collaborative study on DFIT interpretation: Integrating modeling, field data, and analytical techniques. In *the Unconventional Resources Technology Conference, Denver, Colorado, USA*.

McClure, M., Jung, H., Cramer, D., and Sharma, M. (2016). The fracture-compliance method for picking closure pressure from diagnostic fracture-injection tests. *SPE Journal* 21(4): 1321-1339.

McLennan, J. D., & Roegiers, J. C. (1981). Do instantaneous shut-in pressures accurately represent the minimum principal stress. In *USGS Workshop on Hydraulic Fracturing Stress Measurements, Monterey, California, USA*.

Nadimi, S., Forbes, B., Moore, J., & McLennan, J. D. (2020). Effect of natural fractures on determining closure pressure. *Journal of Petroleum Exploration and Production Technology*, 10, 711-728.

Raaen, A. M., Skomedal, E., et al. (2001). Stress determination from hydraulic fracturing tests: the system stiffness approach. *International Journal of Rock Mechanics and Mining Sciences*, 38(4): 529-541

Xing, P., Damjanac, B., Moore, J., & McLennan, J. (2022). Flowback test analyses at the utah frontier observatory for research in geothermal energy (forge) site. *Rock Mechanics and Rock Engineering*, 1-18.

Xing, P., McLennan, J., & Moore, J. (2020). In-situ stress measurements at the Utah frontier observatory for research in geothermal energy (forge) site. *Energies*, 13(21), 5842.

Ye, Z., & Ghassemi, A. (2023a). Assessment of DFIT Analysis Using Laboratory Experiments. *Proceedings of the SPE Annual Technical Conference and Exhibition*, Houston, Texas, October 16-18, 2023, pages 1-15.

Ye, Z., & Ghassemi, A. (2023b). The Cooling Effect on In-situ Stress Determination Using DFIT. *Proceedings of 2023 Geothermal Rising Conference*, Reno, Nevada, October 1-3.

Ye, Z., & Ghassemi, A. (2024). Laboratory Insights on Hydraulic Fracture Closure and Stress Measurement. *Journal of Geophysical Research: Solid Earth (Under Review)*.